Gazi Üniversitesi
Fen Bilimleri Dergisi
PART C: TASARIM VE TEKNOLOJİ

Gazi University
Journal of Science
PART C: DESIGN AND TECHNOLOGY

GU J Sci, Part C, 13(4): 1777-1790 (2025)

Preparation of $CoFe_2O_4$ Nanostructures Modified with ZnS Quantum Dots

Yeliz AKPINAR[1*], Begüm AVCI[2]

[1] *Kırşehir Ahi Evran University, Faculty of Arts and Science, Department of Chemistry, Kırşehir, Turkey*

[2] *Middle East Technical University, Faculty of Arts and Science, Department of Chemistry, Ankara, Turkey*

Article Info

Research article
Received: 22/05/2025
Revision: 21/09/2025
Accepted: 28/10/2025

Keywords

Magnetic Nanoparticle,
Quantum Dots,
Nanotechnology

Makale Bilgisi

Araştırma makalesi
Başvuru:22/05/2025
Düzeltme: 21/09/2025
Kabul: 28/10/2025

Anahtar Kelimeler

Manyetik Nanoparçacık,
Kuantum Noktaları,
Nanoteknoloji

Graphical/Tabular Abstract (Grafik Özet)

A nanostructure with both magnetic and luminescent properties was obtained with a easy methods, and the amide bonds connecting the two nanoparticles (ZnS QDs and SiO_2-MNPs) ensured the strength of the structure. / Kolay bir metod ile hem manyetik özellik hem de lüminesans özelliğe aynı anda sahip elde nanoyapı edilmiş ve iki nanoparçacığı (ZnS QDs ve SiO_2-MNPs) birleştiren amid bağları yapının güçlü olmasını sağlamıştır.

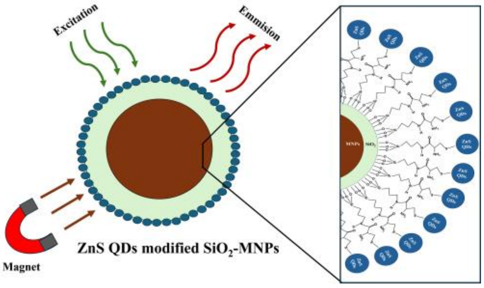

Figure A: *Schematic illustration and properties of the prepared multifunctional nanostructure. /* ***Şekil A:*** *Hazırlanan çok fonksiyonlu nanoyapının şematik gösterimi ve özellikleri.*

Highlights (Önemli noktalar)

- *Both nanostructures (QDs and MNPs) were prepared separately and modified with functional groups. / Her iki nanoyapı (QDs and MNPs) da ayrı ve fonksiyonel gruplar ile modifiye edilerek hazırlandı*
- *The most efficient results were achieved after optimization studies. / Optimizasyon çalışmalarından sonra en verimli sonuç elde edildi.*
- *Characterization studies have shown that the nanostructure is multifunctional. / Karakterizasyon çalışmaları nanoyapının çok fonksiyonlu olduğunu göstermiştir.*

Aim (Amaç): *The aim of this study is to prepare a multifunctional durable nanomaterial with both magnetic and optical (luminescent) properties. / Bu çalışmanın amacı hem manyetik hem de optik (lüminesans) özelliğe sahip çok fonsiyonlu dayanıklı nanomalzemyi hazırlmaktır.*

Originality (Özgünlük): *This study differs significantly from the previous literature by combining the amino group on SiO_2-MNP nanoparticles and the carboxylic acid group on ZnS QDs to form an amide bond using the EDC/NHS coupling reaction. / Bu çalışma, EDC/NHS birleştirme reaksiyonunu kullanarak SiO_2-MNP nanopartikülleri üzerindeki amino grubu ile ZnS QD'leri üzerindeki karboksilik asit grubunu birleştirerek bir amid bağı oluşturması bakımından önceki literatürden önemli ölçüde farklıdır.*

Results (Bulgular): *Characterization studies proved a multifunctional nanostructure exhibiting magnetic and fluorescent properties. XRD patterns revealed ideal crystal sizes. SEM-EDAX images displayed morphological characteristics and elemental composition, while FTIR spectroscopy identified functional groups and amide bonds in the structure. / Karakterizasyon çalışmaları, manyetik ve floresan özellikler sergileyen çok işlevli bir nanoyapıyı ortaya koymuştur. XRD desenleri kristal boyutlarının ideal olduğunu ortaya koymuş, SEM-EDAX görüntüleri morfolojik özellikleri ve elementel bileşimi göstermiş, FTIR spektroskopisi ise yapıdaki fonksiyonel grupları ve amit bağlarını belirlemiştir.*

Conclusion (Sonuç): *ZnS QDs modified SiO_2-MNPs nanostructure is prepared for prospective applications in OLED and photocatalysis. / ZnS QDs modifiye edilmiş SiO_2-MNPs nanoyapısı, gelecekteki OLED ve fotokataliz uygulamaları için hazırlanmıştır.*

---

*Corresponding author, e-mail: yeliz.akpinar@hotmail.com

DOI: 10.29109/gujsc.1704383

GU J Sci, Part C, 13(4): 1777-1790 (2025)

Gazi Üniversitesi
Fen Bilimleri Dergisi
PART C: TASARIM VE TEKNOLOJİ

Gazi University
Journal of Science
PART C: DESIGN AND TECHNOLOGY

http://dergipark.gov.tr/gujsc

Preparation of $CoFe_2O_4$ Nanostructures Modified with ZnS Quantum Dots

Yeliz AKPINAR[1*], Begüm AVCI[2]

[1]*Kırşehir Ahi Evran University, Faculty of Arts and Science, Department of Chemistry, Kırşehir, Turkey*

[2]*Middle East Technical University, Faculty of Arts and Science, Department of Chemistry, Ankara, Turkey*

Article Info

Research article
Received: 22/05/2025
Revision: 21/09/2025
Accepted: 28/10/2025

Keywords

Magnetic Nanoparticle,
Quantum Dots,
Nanotechnology

Abstract

Nanotechnology has gained popularity in the last century, with its applications in daily life making human life easier. Scientists have focused on nanochemistry and nanomaterials, with nanoparticles becoming fundamental tools in material development and production. Magnetic particles are attractive for biomedical, electronics, energy storage, catalyst, and sensor studies due to their magnetic properties. However, metal oxide magnetic particles have shortcomings in optical properties, which can be addressed by creating composites or functionalizing them with different materials. Multifunctional (both luminescent and magnetic) nanostructures were obtained by attaching ZnS QDs to the magnetic particle surface. Differently from studies in the literature, these two different nanostructures were attached by strong amide bonds using the EDC/NHS coupling reaction. The ZnS QDs modifed SiO_2 coated $CoFe_2O_4$ (ZnS QDs modified SiO_2-MNPs) nanostructure is ready for use in future application areas such as OLED and photocatalysis.

ZnS Kuantum Noktaları İle Modifiye Edilmiş $CoFe_2O_4$ Nanoyapılarının Hazırlanması

Makale Bilgisi

Araştırma makalesi
Başvuru:22/05/2025
Düzeltme: 21/09/2025
Kabul: 28/10/2025

Anahtar Kelimeler

Manyetik Nanoparçacık,
Kuantum Noktaları,
Nanoteknoloji

Öz

Nanoteknoloji, günlük yaşamdaki uygulamalarıyla insan hayatını kolaylaştırarak, son yüzyılda popülerlik kazanmıştır. Bilim insanları nanokimyaya ve nanomateryallere odaklanmış, nanoparçacıklar malzeme geliştirme ve üretiminde temel araçlar haline gelmiştir. Manyetik parçacıklar, manyetik özellikleri nedeniyle biyomedikal, elektronik, enerji depolama, katalizör ve sensör çalışmaları için çekicidir. Ancak metal oksit manyetik parçacıkların optik özelliklerinde eksiklikleri vardır; bu da kompozitler oluşturularak veya farklı malzemelerle fonksiyonelleştirilerek giderilebilir. Bu çalışmada, çok işlevli (hem lümisent ışıma yapan hem de manyetik) özelliklere sahip nanoyapılar, manyetik parçacık yüzeyine ZnS kuantum noktaları eklenerek elde edilmiştir. Literatürdeki çalışmalardan farklı olarak, bu iki farklı nanoyapı, EDC/NHS birleştirme reaksiyonu kullanılarak güçlü amid bağlarıyla birleştirilmiştir. ZnS QD modifiye edilmiş SiO_2 kaplı $CoFe_2O_4$ (ZnS QDs modifiye edilmiş SiO_2-MNPs) nanoyapısı, OLED ve Fotokataliz gibi gelecekteki pek çok uygulama alanlarında kullanıma hazırdır.

1. INTRODUCTION (GİRİŞ)

Recently, the use of nanoparticles in scientific and technological fields has increased rapidly. Magnetic particles have attracted great attention in medical and technological applications thanks to their acceptable biocompatibility, high magnetic properties, various surface modifications, and easy synthesis methods [1]. The magnetic nanoparticles can be classified as magnetic metallic nanoparticles (such as Co, Fe), magnetic alloy nanoparticles (such as Fe–Co, Fe–Ni, Fe–Pt, Co–Pt, Co–Ni), and metal oxides (such as Fe_3O_4, γ-Fe_2O_3), $NiFe_2O_4$, $MnFe_2O_4$, $CoFe_2O_4$, $NiCo_2O_4$, NiO, Co_3O_4) [2], [3]. The important shortcoming of magnetic particles is their lack of optical properties. In catalyst and sensor studies, the lack of surface plasmon resonance (SPR), conductivity, or luminescence properties becomes a disadvantage in characterization and application processes. To overcome this disadvantage, the surfaces of magnetic particles can be modified with SPR active particles or luminescent dyes and quantum particles. Conductivity property is especially necessary in

---

*Corresponding author, e-mail: yeliz.akpinar@hotmail.com

DOI: 10.29109/gujsc.1704383

electronic applications [4]. Magnetic particles can be synthesized using physical, chemical, and biological methods. Co-precipitation is the most common technique, where a metal salt is synthesized in a controlled environment. Thermal decomposition, hydrothermal, and microwave techniques can produce varying shapes, sizes, and compositions of magnetic particles. In comparison to co-pecipation methods, these three methods are more expensive, more time consuming, and require special equipment and devices [5]. Therefore, the co-precipitation method was used in this study.

The scientific field widely uses quantum particles with sizes smaller than 10 nm due to their photochemical properties. These particles significantly increase the analytical performance, selectivity, and sensitivity of biosensors. Semiconductivity and luminescence properties have made these particles an important tool for electrochemical applications, solar energy, and energy and data storage studies. Quantum particles can be prepared in two main categories: metallic or metallic alloys, such as (CdS) ZnS, (CdSe) ZnS, (CdSe) CdS, and (InAs) CdS; and organic-based particles, including carbon quantum particles and carbon nanotubes. ZnS quantum particles are preferred for OLED device design and photocatalyst studies due to their strong and stable fluorescent luminescence properties, a wide band gap (band gap ≈ 3.6–3.7 eV), high conductivity, good durability under UV light, non-toxicity, cheapness, accessibility, and their ability to act as a good electron carrier [6], [7]. There are different quantum dot preparation methods. Specifically, when examining the preparation of ZnS QDs used in this study, different methods were used depending on the purpose. Dile et al. used the hydrothermal method, Mandal et al. used the sol-gel method, Guaddarzi et al. used microwave assisted decoposition, and Bhushan et al. used the thermal decoposition method [8], [9], [10], [11]. While these methods allow for controllable size and shape optimization, their disadvantages include the need for expensive equipment and the use of organic surfactants and chemicals. Specifically, the ZnS QDs used in this study were prepared by chemical precipitation. This method is inexpensive, environmentally friendly, hydrophilic, and fast. Its disadvantage is that optimizing shape and size is quite difficult [12].

Organic light-emitting diode (OLED) represents the high point of automation for display and lighting applications, owing to its advantageous characteristics such as wide viewing angle, rapid response time, self-emissive properties, flat lightweight design, low production costs, extensive luminous display area, flexibility, and low power consumption [13]. The nanoparticles exhibit distinctive features and play numerous functions in OLEDs, including enhancement of carrier injection capabilities, local surface plasmonic resonance, light scattering, and magnetic field effects [14]. Magnetic nanoparticles have applications in optics owing to their distinctive magneto-optical properties in a magnetic field, including optical anisotropy, field-dependent transmission, and birefringence [15]. In literature, there are too many OLED applications by using magnetic nanoparticles such as Fe_3O_4 and, $CoFe_2O_4$ [16], [17]. Studies indicate that solution-processed tandem OLEDs are limited by less efficient polymer-based emitters which are basic materials for these applications, while phosphorescent, light scattering and thermally triggered delayed fluorescent materials are preferred for high efficiency and longevity, while inorganic colloidal quantum dots are viable candidates [18]. Recent studies in OLED applications have shown widespread use of quantum dots due to their efficient optical properties. Examples of inorganic or organic quantum dots include Al-ZnO nanohybrids, graphene oxide, and CdSe/ZnS [18], [19], [20]. The combined use of magnetic and optical properties is crucial for increasing OLED efficiency. Noori et al. developed a ZnQ-coated $NiFe_2O_4$ material for this purpose and achieved desirable results [21]. In a similar study, Lian et al. used graphene oxide, which has high electroluminescence properties, in combination with Fe_3O_4 nanoparticles in OLED device design and achieved high efficiency [22].

Another area where nanoparticles are used is photocatalytic applications. They are widely used in both energy (water splitting, etc.) and environmental (dye degradation, wastewater treatment) areas. The ability to coat surfaces with different catalytic molecules and particles, and to store the magnetic separation procedure, making the magnetic type easy to reuse, makes it functional in these applications [23]. The lack of optical properties (plasmonic and electroluminescence), which is a disadvantage in other applications, makes magnetic particles inadequate for this purpose. Karimi et al. designed Fe_3O_4@ZnS QDs and Fe_3O_4@NPs as photocatalysts in organic dye degradation study and achieved high photodegregation percentages [24]. In the study of Palanisamy et al., they used a ZnS-WO_3-$CoFe_2O_4$ nanohybrid structure as a catalyst for the photodegradation of methylene blue and reported a higher degradation effect in shorter irradiation time due to the synergetic effect of both quantum dots and magnetic nanoparticles [25]. In the study of Chang et al., ZnS-encapsulated $CoFe_2O_4$ nanoparticles used as photocatalysts increased the water splitting efficiency, and this structure was shown to have stability to obtain 87% efficiency even after three reuses [26].

In previous sections, the use of magnetic nanoparticle-quantum dot nanocomposite structures in OLED and photocatalyst studies, where they are widely used, has been detailed. This study's prepared nanostructure can anticipate application in diverse fields. Literature studies have identified applications where magnetic nanoparticle-quantum dot structures are used: dermatoglyphics and anti-counterfeiting applications (Fe_3O_4/ZnS hybrid), magnetic hyperthermia (biomedical applications) ($CoFe_2O_4$/ZnS), sensors (Fe_3O_4 MNPs and Mn^{2+}:ZnS QDs), etc. [27], [28], [29].

In this study, $CoFe_2O_4$ NPs will be synthesized by the coprecipitation method, and their surfaces were coated with silica. ZnS quantum particles were prepared by the chemical precipitation method, and their surfaces were modified with L-cysteine. L-cysteine-modified ZnS quantum particles were attached to SiO_2-$CoFe_2O_4$ NPs surfaces by EDC/NHS coupling reaction [12], [30]. The prepared nanomaterial was characterized and made ready for future studies.

2. MATERIALS AND METHODS (MATERYAL VE METOD)

2.1. Preparation of Amine Modified Silica-Cobalt Ferrite Magnetic Nanoparticles (SiO_2-MNPs) (Amin Modifiye Silika-Kobalt Ferrit Manyetik Nanopartiküllerin (SiO_2-MNP'ler) Hazırlanması)

$CoFe_2O_4$ nanoparticles were prepared by the co-precipitation method [31], and the basic scheme is given in Figure 1a. The solution of $CoCl_2$ and $FeCl_3$ salts was prepared in a flask at a mole ratio of 1:2 and mixed in NaOH solution at 80°C for one hour. The resulting black particles were collected with the help of a magnet, and magnetic washing was performed 3 times with a mixture of ethanol, 2-propanol, methanol, and water. Finally, it was dispersed in deionized water. The Stöber technique was used to encapsulate $CoFe_2O_4$ nanoparticles with silica shells (Figure 1b). Uncoated magnetic nanoparticles were evenly distributed in water .

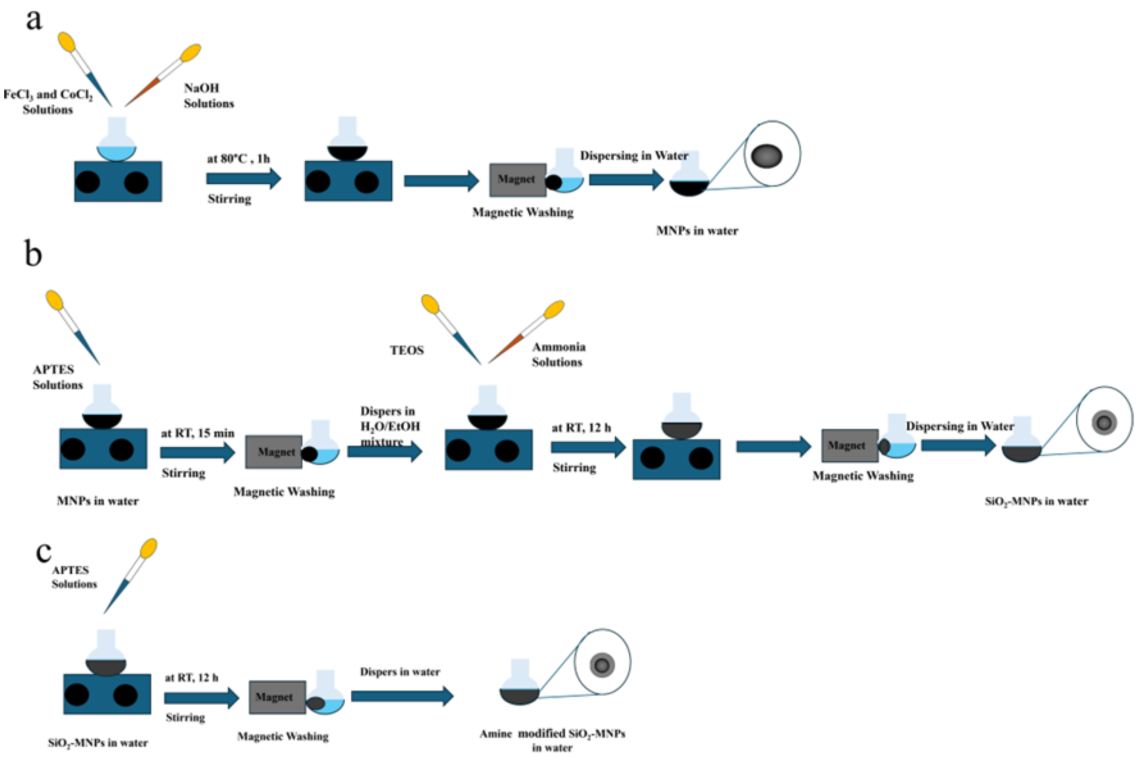

Figure 1. Scheme of a) preparation MNPs, b) encapsulation with silica shell, c) amine modification SiO_2-MNPs procedure (a) MNP'lerin hazırlanması, b) silika kabukla kapsülleme, c) SiO_2-MNP ların amin modifikasyonu prosedürünün şeması)

A concentration of 1 millimolar of (3-aminopropyl) triethoxysilane (APTES) was introduced into the solution and thoroughly stirred for a duration of 15 minutes at room temperature. Via magnet, a magnetic washing procedure was applied to nanoparticles to remove unbounded APTES molecules. These particles were then dispersed in a combination of deionized water and ethanol, with a ratio of 1 part water to 4 parts ethanol. After adding tetraethyl orthosilicate (TEOS) and ammonia to the solution, the mixture was stirred for a duration of 12 hours. $CoFe_2O_4$ nanoparticles coated with silica (SiO_2-MNPs) were applied to three rounds of washing using ethanol, methanol, and ionized water, followed by immersion in deionized water. Then, SiO_2-MNPs were modified with amine, and Figure 1c illustrates the basic scheme of this procedure. Firstly, SiO_2-MNPs were distributed in ethanol. Later, APTES was added to this solution, and after 12 hours of mixing, the particles were rinsed four times with ethanol, methanol, and water to eliminate environmental contamination. Finally, a stock solution was prepared by dispersing SiO_2-MNPs in 50 mL DI water.[31]

2.2. Preparation of ZnS Quantum Dots (ZnS Kuantum Noktalarının Hazırlanması)

The chemical precipitation method was used to prepare ZnS QDs. Subsequently, the following methods were carried out [12], [30] A summary of the procedure is given in Figure 2. The obtained materials were labeled as Sample 1, Sample 2, Sample 3, and Sample 4.

Sample 1: A 5.0-mL portion of a solution containing a 0.5 molar concentration of zinc acetate was prepared, and then 25 mg of L-cysteine was added to this solution. The solution's pH was modified to 10 by using the NaOH solution. After 15 minutes of stirring, a 1.0 M solution of Na_2S was added to this solution in droplets, with a volume of 2.5 mL. The mixture was stirred for an additional 30 minutes. A solution resembling milk in appearance and white color was produced. The particles were rinsed with water and brought up to a final volume of 12.0 mL using a centrifuge operating at 4000 rpm for 10 minutes. The same procedure was applied for the others. The pH values and concentrations of both L-cysteine and Na_2S were optimized. The parameters are given in Table 1.

2.3. Coupling of SiO_2-MNPs with ZnS Quantum Dots (SiO_2-MNP'lerin ZnS Kuantum Noktalarıyla Birleştirilmesi)

Amine-modified silica coated $CoFe_2O_4$ nanoparticles (SiO_2-MNPs) were attached to the L-cysteine modified ZnS quantum dots using an EDC/NHS coupling reaction. The procedure scheme is given in Figure 3.

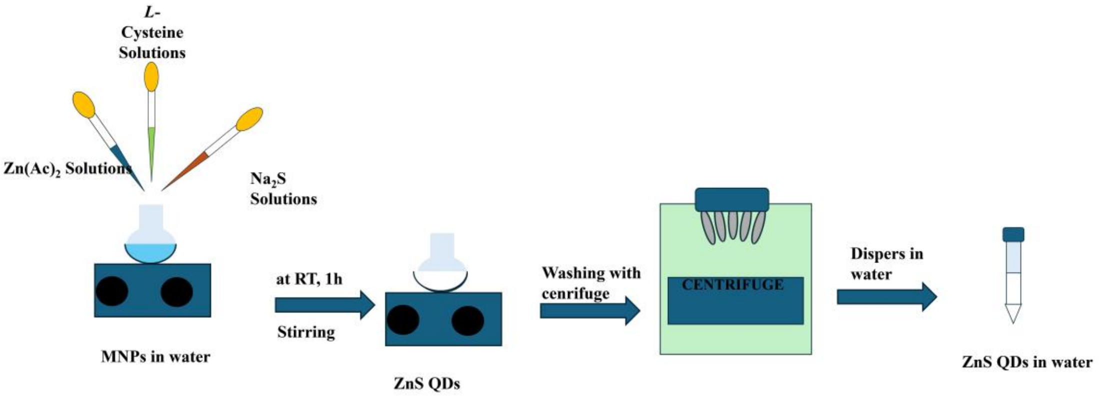

Figure 2. Basic scheme of preparation of L-cysteine modified ZnS QDs procedure (L-cysteine modified ZnS QDs ların hazırlanması prosedürünün genel şeması)

Table 1. Optimization parameters of preparation of ZnS QDs (ZnS QD'lerin hazırlanması için optimizasyon parametreleri)

Sample	pH	L-cysteine (mg)	Na_2S (M)
Sample 1	10	25	1.0
Sample 2	7	25	0.5
Sample 3	7	25	1.0
Sample 4	7	12.5	0.5

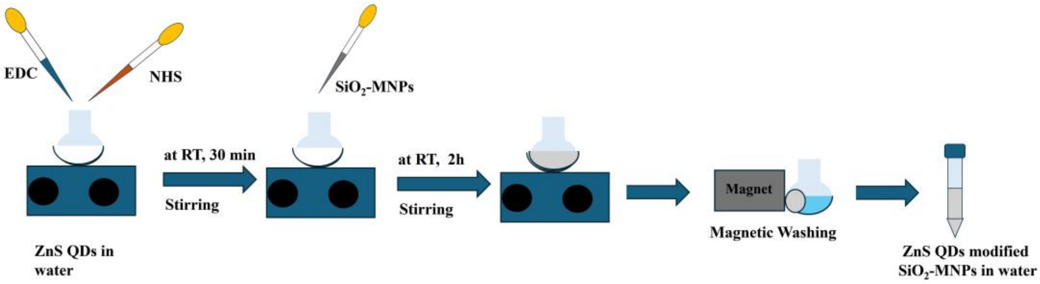

Figure 3. Basic scheme of coupling procedure between SiO_2-MNPs and ZnS Quantum Dots (SiO_2-MNP'ler ile ZnS Quantum Dot arasındaki bağlantı prosedürünün temel şeması)

A dilution optimization study was carried out for the prepared ZnS QDs solution and the coupling procedure was carried out with the ratio of 1:27 (ZnS QDs solution: water, v:v), which gave the highest emission efficiency. A 530 µl portion of 0.5 mM EDC and that of 0.25 mM NHS solutions were added to the 1.0 Ml ZnS QDs solution, which was modified by L-cysteine and this mixture was stirred for 30 min. After that, 5.0 mL of SiO_2-MNPs solution (which was prepared by diluting 3.0 mL stock solution to 5.0 mL with DI water) was added to the previous solution and stirred for 2 h at 600 rpm. After magnetic washing three times with water, the ZnS QDs modified SiO_2-MNPs were dispersed in 3.0 mL DI water [31]. For the optimization studies, different amounts of ZnS QDs (0.25 mL, 0.5 mL, and 1.0 mL) were used for coupling reactions, and ZnS QDs modified SiO_2-MNPs-1, ZnS QDs modified SiO_2-MNPs-2, and, ZnS QDs modified SiO_2-MNPs-3, solutions were obtained, respectively.

3. RESULTS (BULGULAR)

Fluorescence measurements were obtained after the solutions prepared with the method described above were diluted to a ratio of 1:9. The device had its excitation value set to 320 nm when it was turned on. The resulting spectra is shown in Figure 4.

According to the optimization results, low yield was obtained when the reaction was carried out in a basic medium (Sample 1, green line). After the solution was neutralized, the highest yield was obtained in the experiment prepared with the same zinc and sulfide concentrations (sample 2, red line). In Sample 3 (Sample 3, yellow line)., the amount of Na_2S was increased, and the parameters in Sample 2 were used. But a significantly lower yield was obtained compared to Sample 2. Finally, a trial was conducted by reducing the amount of L-cysteine in the surface coating material (Sample 4, blue line). The best result was obtained comparing Sample 2, so it was decided to continue with Sample 2. Then, it was determined at what concentration the ZnS solution should be used. For this purpose, the prepared raw ZnS solution was diluted in different proportions and fluorescence measurements were taken. The excitation value on the device was set to 320 nm.

The optimization work done at this stage is given in Figure 5. QD samples were prepared at a ratio of 1:9 (ZnS QDs solution: water). In this study, ratios of 1:9 (red line), 1:18 (green line), 1:27 (orange line), and 1:54 (blue line) were tested. The trend in the spectra is in line with the literature information. As the dilution increased, the fluorescence efficiency increased, but it was observed that the efficiency decreased at the most dilute ratio of 1:54. For this reason, the 1:27 dilution ratio (orange line) with the highest efficiency was used in the next part of the study.The reason for this result is that the photoluminescence efficiency of quantum dots decreases with increasing concentration due to non-radiative energy transfer, self-absorption effects, particle aggregation, surface imperfections, and inner filter effects. This results in quenching without light emission, reabsorbing photos, and increasing non-radiative transitions. Excessive density also heightens surface imperfections, leading to increased non-radiative transitions. The inner filter effect further absorbs excitation light, compromising emission uniformity and highlighting the importance of reducing concentrations for optimal fluorescence intensity [32], [33].

The excitation value on the device was set to 320 nm. The optimum result (ZnS QDs modified SiO_2-MNPs -1) was obtained when 0.25 mL of L-cysteine modified ZnS quantum dot solution was added to the reaction medium (Figure 6). Here, it was observed that the emission efficiency decreased as the quantum dot density on the SiO_2-MNPs surface increased, for similar reasons as in the dilution optimization studies. Also there are not any significant emission peaks that belong to SiO_2-MNPs and MNPs.

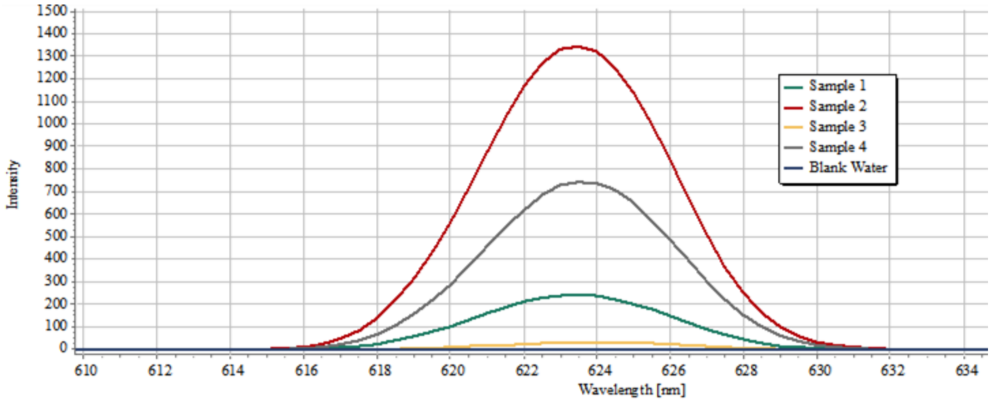

Figure 4. Fluorescence (emission) spectra of L-cysteine-coated ZnS QDs solutions (L-sistein kaplı ZnS kuantum parçacıklarının floresan (emisyon) spektrumları)

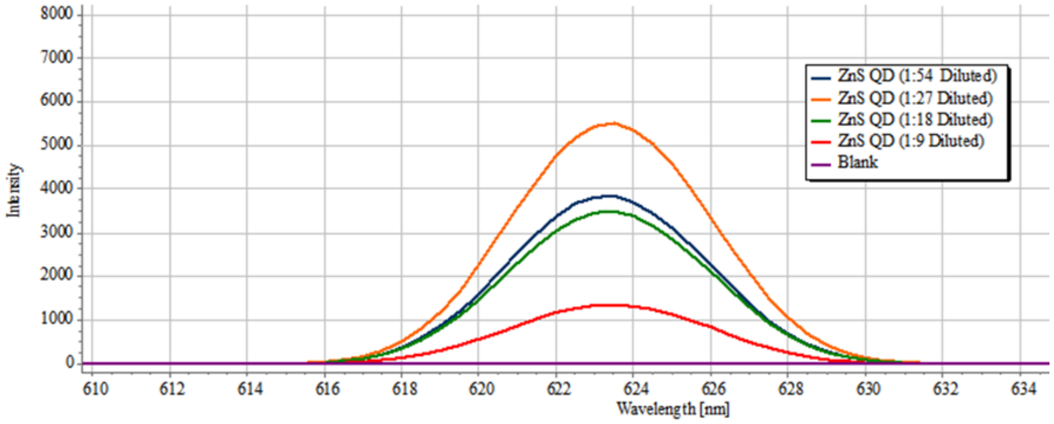

Figure 5. Fluorescence spectra of ZnS QDs solutions with different dilution ratio. (Farklı seyreltme oranlarına sahip ZnS QD çözeltilerinin floresan spektrumları.)

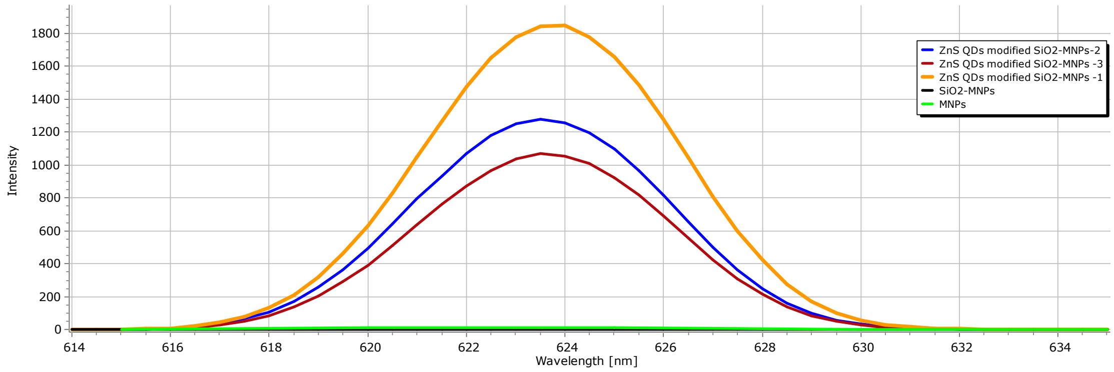

Figure 6. Fluorescence spectra of ZnS QDs modified SiO_2-MNPs -1, ZnS QDs modified SiO_2-MNPs -2, and ZnS QDs modified SiO_2-MNPs-3, as a result of the coupling reaction using different amounts of ZnS QDs solution 0.25 mL, 0.5 mL, and 1.0 mL, respectively. In addition, fluorescence spectra of MNPs and SiO_2-MNPs, (Sırasıyla 0.25 mL, 0.5 mL, and 1.0 mL farklı miktarlarda ZnS QDs çözeltisi kullanılarak gerçekleştirilen birleştirme reaksiyonu sonucunda ZnS QDs modifiye SiO_2-MNPs -1, ZnS QDs modifiye SiO_2-MNPs -2 ve ZnS QDs modifiye SiO_2-MNPs-3 floresans spektrumları. Ek olarak MNPs ve SiO2-MNPs Floresans spektrumları.)

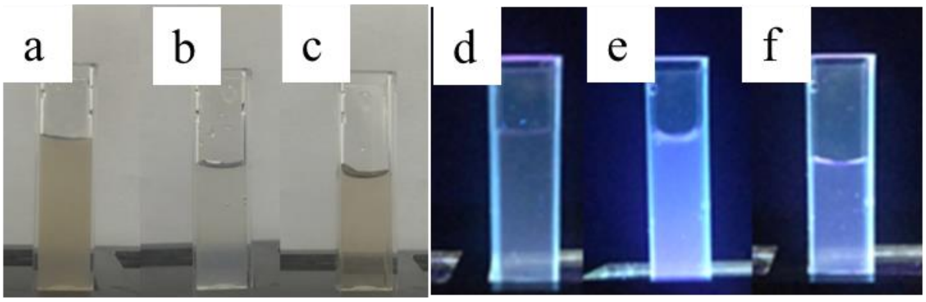

Figure 7. Under solar light a) SiO_2-MNPs solutions, b) ZnS QDs solutions, and c) ZnS QDs modified SiO_2-MNPs; Under UV light: d) SiO_2-MNPs solutions, e) ZnS QDs solutions, and f) ZnS QDs modified SiO_2-MNPs (Güneş ışığı altında a) SiO_2-MNPs çözeltileri, b) ZnS QDs çözeltileri, c) ZnS QDs modifiye SiO_2-MNPs; UV ışığı altında d) SiO_2-MNPs çözeltileri, e) ZnS QDs çözeltileri, and f) ZnS QDs modifiye SiO_2-MNPs)

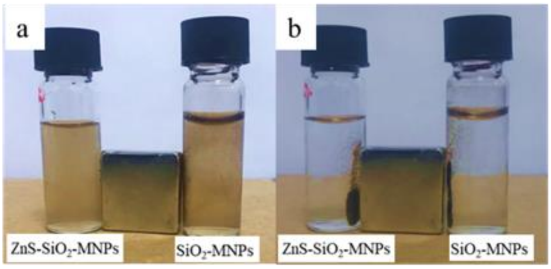

Figure 8. a) 0 seconds, b) 30 seconds after the magnet is placed next to it, both ZnS QDs modified SiO_2-MNPs and unmodified SiO_2-MNPs solutions (mıknatıs yanına yerleştirildikten a) 0 saniye, b) 30 saniye sonra hem ZnS QDs modifiye SiO_2-MNPs hem de modifiye edilmemiş SiO_2-MNPs çözeltilerinin görünümü)

According to Figure 7, a and d, the amine-modified MNP did not show any emission under UV light, while c and f showed that the emission is due to the surface of the MNP being modified with ZnS QDs.

According to Figure 8, both ZnS QDs modified SiO_2-MNPs and unmodified SiO_2-MNPs were collected by the magnet 30 seconds after being placed near the magnet. The fact that there were no particles in the supernatant remaining after the particles were collected by the magnet in the ZnS QDs modified SiO_2-MNPs solution indicates that the attachment of ZnS and MNPs to each other was successful.

At Figure 9, FTIR spectra are given for the prepared MNPs ($CoFe_2O_4$) (green line), SiO_2-MNPs (red line), and ZnS QDs modified SiO_2-MNPs (blue line). With this characterization technique, the structural skeleton of ZnS QDs modified SiO_2-MNPs, that is, the bonds between elements and the specific peaks of the formed functional groups, were shown. For three spectra, the peak at 580.90 cm^{-1} indicates the Co-O interaction in the octahedral structure, which proves $CoFe_3O_4$ formation [34]. Both the peaks at 799.83 and 802.64 cm^{-1} belong to the bending motion of the N-H bond, indicating the presence of L-cysteine (it covers the ZnS surface) in the blue spectrum and the cobalt ferrite surface being modified with amine in the red spectrum, respectively. Similarly, the characteristic N-H bending vibration peaks between 1647 cm^{-1} and 1540 cm^{-1} indicate the presence of the amine group in both the amine-modified silica-coated cobalt ferrite particle and the ZnS QDs bonded amine-modified silica-coated cobalt ferrite particle. In addition, the broad band at 1096.49 cm^{-1} in both spectra belongs to the Si-O bond and indicates the presence of silica on the particle surface; as a result, silica shell formation was proved [31]. In addition, the broad band at 1635.64 cm^{-1} in the blue spectrum belongs to the amide II bond of the amide formed during the coupling reaction. Peaks in both spectra (blue and red) between 2900-3420 cm^{-1} are further evidence of the $-NH_2$ group [35]. This result shows that the reaction has taken place. The peak at 852.25 cm^{-1} in the blue spectrum of the silica-coated cobalt ferrite particle modified with ZnS-bonded amine shows the stretching vibration of the Zn-S bond [4].

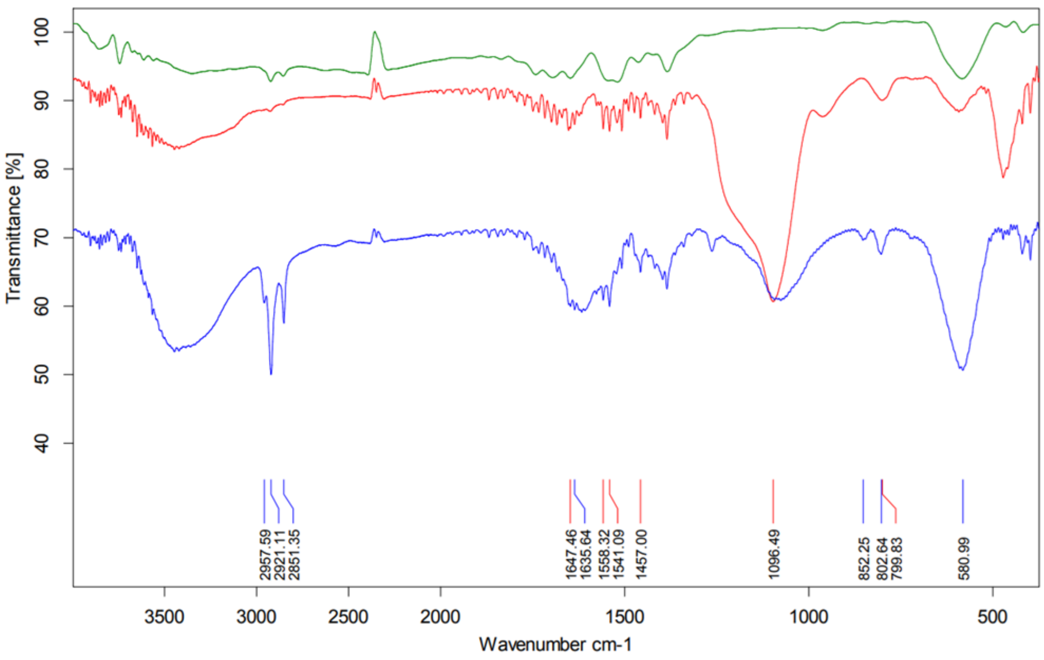

Figure 9. FTIR spectra of MNPs (green line), SiO_2-MNPs (red line) and ZnS QDs modified SiO_2-MNPs (blue line), respectively (Sırasıyla MNP'lerin (yeşil çizgi), SiO_2-MNP'lerin (kırmızı çizgi) ve ZnS QD'lerle modifiye edilmiş SiO_2-MNP'lerin (mavi çizgi) FTIR spektrumları)

Powder X-ray diffraction experiments were conducted with the Rigaku Mini-Flex X-ray powder Diffractometer (XRD) source of Cu-Kα line (λ=1,54056 Å) to get the structural data. The crystallinity of the formed cobalt ferrite was assessed using X-ray diffraction (XRD), yielding patterns within the 20–70° range at 2 theta degrees. Figure 10 illustrates the X-ray diffraction pattern of the generated MNPs and SiO_2-MNPs samples. The synthesized $CoFe_2O_4$ (MNPs) exhibited diffraction peaks located at (2 theta) of 30.01°, 35.88°, 43.11°, 57.16 °, and 62.88 ° corresponding to the (220), (311), (400), (511), and (440) planes, which aligned with the standard data for $CoFe_2O_4$ (JCPDS no: 03–0864), indicating that its structure was classified as a single crystalline phase. The five peaks were utilized to ascertain the size of the crystals of the samples employing Scherrer's formula and the average of crystalline size of $CoFe_2O_4$ was calculated as 15.66±0.97 nm (Anchal et al., 2024). The diffraction peaks of silica-coated samples are comparable to those of MNPs and SiO_2-MNPs, with no extra peaks observed, thereby verifying the presence of amorphous silica [37].

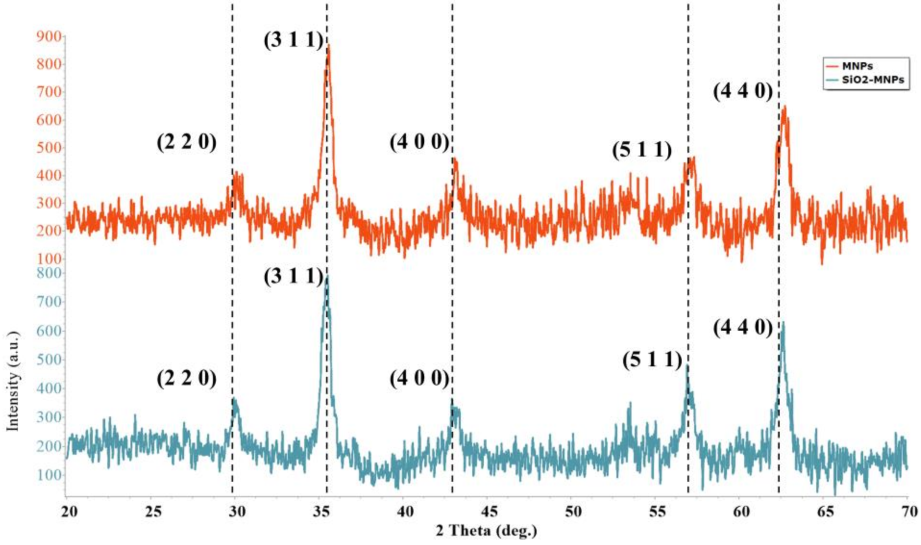

Figure 10. The XRD pattern of SiO_2-MNPs (blue line) MNPs (red line), respectively (Sırasıyla SiO_2-MNPs (mavi çizgi), MNP'lerin (kırmızı çizgi) XRD desenleri)

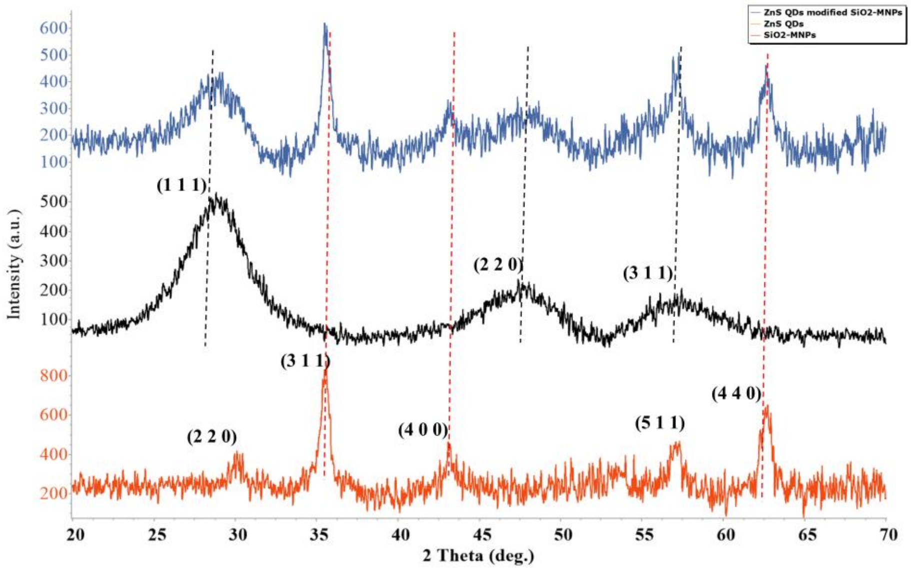

Figure 11. The XRD pattern of SiO_2-MNPs (red line) ZnS QDs (black line), and ZnS QDs modified SiO_2-MNPs (blue line,) respectively. (Sırasıyla SiO_2-MNPs (kırmızı çizgi), MNP'lerin (kırmızı çizgi) XRD desenleri)

Figure 11 illustrates the X-ray diffraction (XRD) pattern for ZnS QDs (black line). Three significant peaks were found at 2θ angular locations of 28.70°, 47.71°, and 56.90°. The peaks matched the planes of crystallography (1 1 1), (2 2 0), and (3 1 1) of the zinc blende (cubic) phase of ZnS, respectively. These results align with the information shown in JCPDS card number 05-0566. The Scherrer equation can be used to determine the size of ZnS QDs over three planes. The predicted crystal size is 2.02±0.06 nm [38], [39]. Additionally, when comparing the XRD patterns of the SiO_2-MNPs, ZnS QDs, and ZnS-modified SiO_2-MNPs given in Figure 11, the pattern of the ZnS-modified SiO_2-MNPs shows planes belonging to both the SiO_2-MNPs and the ZnS QDs. This result indicates that two different types of particles are stably bound to each other and their crystal structures remain unchanged.

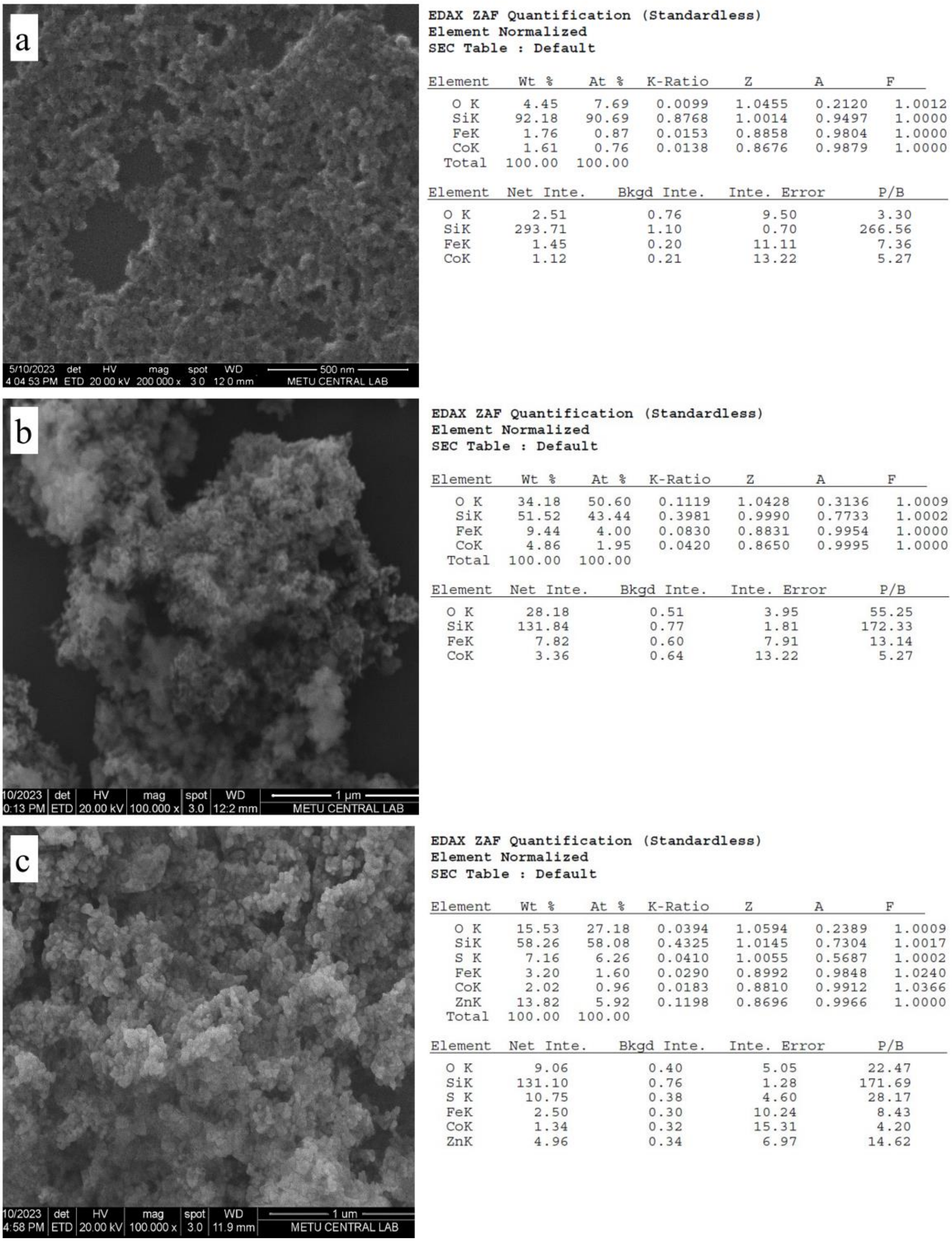

```
EDAX ZAF Quantification (Standardless)
Element Normalized
SEC Table : Default

Element   Wt %    At %   K-Ratio     Z        A        F
   O K     4.45    7.69   0.0099   1.0455   0.2120   1.0012
   SiK    92.18   90.69   0.8768   1.0014   0.9497   1.0000
   FeK     1.76    0.87   0.0153   0.8858   0.9804   1.0000
   CoK     1.61    0.76   0.0138   0.8676   0.9879   1.0000
  Total  100.00  100.00

Element  Net Inte.    Bkgd Inte.   Inte. Error      P/B
  O K        2.51          0.76          9.50         3.30
  SiK      293.71          1.10          0.70       266.56
  FeK        1.45          0.20         11.11         7.36
  CoK        1.12          0.21         13.22         5.27
```

```
EDAX ZAF Quantification (Standardless)
Element Normalized
SEC Table : Default

Element   Wt %    At %   K-Ratio     Z        A        F
   O K    34.18   50.60   0.1119   1.0428   0.3136   1.0009
   SiK    51.52   43.44   0.3981   0.9990   0.7733   1.0002
   FeK     9.44    4.00   0.0830   0.8831   0.9954   1.0000
   CoK     4.86    1.95   0.0420   0.8650   0.9995   1.0000
  Total  100.00  100.00

Element  Net Inte.    Bkgd Inte.   Inte. Error      P/B
  O K       28.18          0.51          3.95        55.25
  SiK      131.84          0.77          1.81       172.33
  FeK        7.82          0.60          7.91        13.14
  CoK        3.36          0.64         13.22         5.27
```

```
EDAX ZAF Quantification (Standardless)
Element Normalized
SEC Table : Default

Element   Wt %    At %   K-Ratio     Z        A        F
   O K    15.53   27.18   0.0394   1.0594   0.2389   1.0009
   SiK    58.26   58.08   0.4325   1.0145   0.7304   1.0017
   S K     7.16    6.26   0.0410   1.0055   0.5687   1.0002
   FeK     3.20    1.60   0.0290   0.8992   0.9848   1.0240
   CoK     2.02    0.96   0.0183   0.8810   0.9912   1.0366
   ZnK    13.82    5.92   0.1198   0.8696   0.9966   1.0000
  Total  100.00  100.00

Element  Net Inte.    Bkgd Inte.   Inte. Error      P/B
  O K        9.06          0.40          5.05        22.47
  SiK      131.10          0.76          1.28       171.69
  S K       10.75          0.38          4.60        28.17
  FeK        2.50          0.30         10.24         8.43
  CoK        1.34          0.32         15.31         4.20
  ZnK        4.96          0.34          6.97        14.62
```

Figure 12. SEM images and EDAX results of a)MNPs, b) SiO_2-MNPs, c) ZnS QDs modified SiO_2-MNPs
(a) MNP'lerin, b) SiO_2-MNP'lerin, c) ZnS QD'ler ile modifiye edilmiş SiO_2-MNP'lerin SEM görüntüleri ve EDAX sonuçları)

The SEM image in Figure 12a shows that the $CoFe_2O_4$ NPs (MNPs) structure is formed at nanoscale. Simultaneous EDAX measurement proves the presence of cobalt iron and oxygen. Si is also seen in the EDAX table of MNPs (Figure 12 a). The image in Figure 12b is morphologically different from Figure 12a. Since the samples were prepared on silicon wafers, The white layer surrounding the particles shows the silica shell structure and the size of the newly formed particles is larger. EDAX measurements also show the elemental content of the nanostructure. The SEM image shown in Figure 12c is of SiO_2-MNPs modified with ZnS QDs. Morphologically, it has a different structure and more agglomeration than the bare silica-coated particles. In addition, simultaneous EDAX measurements prove that the presence of Zn, S, Co, Fe, O and Si elements proves the formation of the intended nanostructure

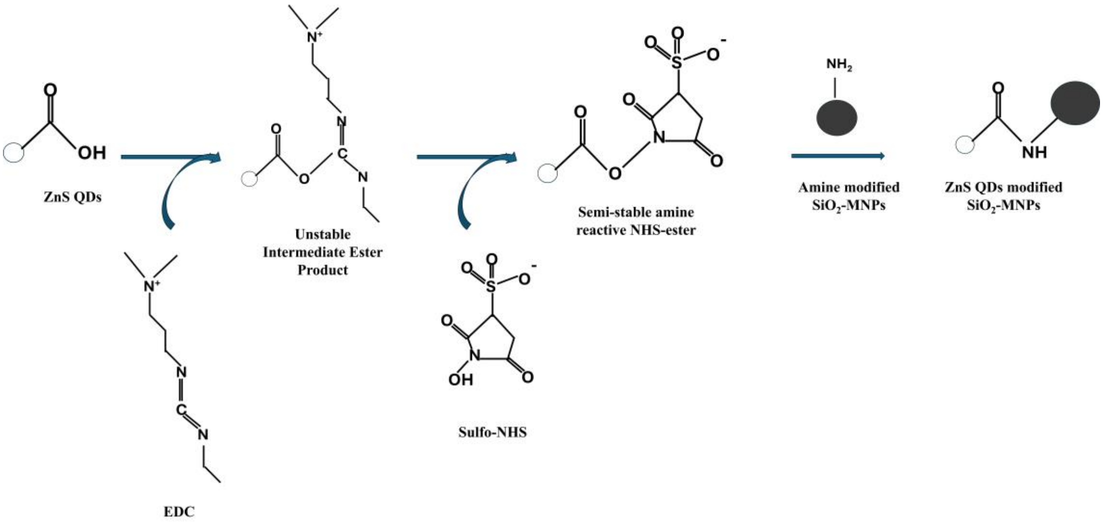

Figure 13. Scheme of EDC/NHS coupling reaction (EDC/NHS birleşme reaksiyonunun şematik gösterimi)

XRD, SEM-EDAX, FTIR spectroscopy, and fluorimetry spectroscopy results indicate that ZnS QDs and SiO_2-coated $CoFe_2O_4$ magnetic nanoparticles bind to the surface. The QDs remain attached to the magnetic nanoparticle despite the magnetic washing process, demonstrating the strength and stability of the bond For this purpose, the EDC/NHS coupling reaction method was chosen for nanomaterial preparation, differently from similar studies at literature.

This study has been differed from studies in literature by the utilization of the EDC/NHS coupling reaction. The amino group on the (SiO_2-MNPs) nanoparticles and the carboxylic acid group in the L-cysteine merge in the reaction to form an amide bond. Similar studies exist in literature; this study distinguishes itself by covalently bonding ZnS and SiO_2-MNPs nanostructures, achieving a more stable structure (amide bonds) and maintaining the properties of two different nanoparticles together. There is a schematic illustration given in Figure 13. The EDC/NHS coupling procedure was chosen for this aim, which forms amide bonds between carboxylic acids and amines and is widely used in material science due to its convenience, simplicity, adaptability, biocompatibility, and application in aqueous solutions. Its absence of chemical extension during functionalization, strong amide bonds, and its biocompatibility make this method attractive [40].

By selecting co-precipitation and chemical precipitation methods, the desired particles were obtained quickly and easily without requiring specialized equipment or expensive/hazardous chemicals. Characterization studies proved that the targeted particles have been prepared. The reasons for preferring ZnS QDs and $CoFe_2O_4$ nanoparticles in this study are that these particles have low toxic effects, high magnetic and optical properties, cheap and available precursors, and easy preparation

4. CONCLUSIONS (SONUÇLAR)

In this study, nanostructures with multiple properties were created. By combining the magnetic properties of $CoFe_2O_4$ NPs with the optical properties of ZnS QDs, a single structure with richer properties, higher efficiency, and a wider range of applications was achieved. By coating the magnetic particles with silica, the magnetic core was made more stable against oxidation and suitable surface conditions were provided for the attachment of ZnS QDs. Characterization studies revealed a multifunctional, optimized nanostructure with both magnetic and fluorescent properties. Fluorimetry measurements prove 624 nm emission both ZnS QDs and ZnS QD-modified SiO_2-MNPs. XRD patterns demonstrated that this nanostructure had appropriate crystal size (15.66 ±0.97 and 2.02 ±0.06 nm) and lattice properties. SEM-EDAX images demonstrated the morphological nanostructure formation and illustrated the structure's elemental formation. FTIR Spectroscopy provided information about the functional groups formed in the structure and the covalent bonds that indicate the combination. ZnS QD modified SiO_2-MNPs are prepared for use in being promised optoelectronic, catalyst, and biomedical applications for future work.

ACKNOWLEDGMENTS (TEŞEKKÜR)

This work was supported by the Research Fund of Kirsehir Ahi Evran University through Project FEF.A4.22.001. We are grateful to Prof. Dr. Ayşen YILMAZ (METU, Department of Chemistry) for her support in the XRD measurements and Prof. Dr. Mürvet VOLKAN (METU, Department of Chemistry) for her support.

DECLARATION OF ETHICAL STANDARDS (ETİK STANDARTLARIN BEYANI)

The author of this article declares that the materials and methods they use in their work do not require ethical committee approval and/or legal-specific permission.

Bu makalenin yazarı çalışmalarında kullandıkları materyal ve yöntemlerin etik kurul izni ve/veya yasal-özel bir izin gerektirmediğini beyan ederler.

AUTHORS' CONTRIBUTIONS (YAZARLARIN KATKILARI)

***Yeliz AKPINAR*:** She conducted the experiments, analyzed the results and performed the writing process.

Deneyleri yapmış, sonuçlarını analiz etmiş ve makalenin yazım işlemini gerçekleştirmiştir.

***Begüm AVCI*:** She performed the experiments, and the writing process.

Deneyleri yapmış ve makalenin yazım işlemini gerçekleştirmiştir.

CONFLICT OF INTEREST (ÇIKAR ÇATIŞMASI)

There is no conflict of interest in this study.

Bu çalışmada herhangi bir çıkar çatışması yoktur.

REFERENCES (KAYNAKLAR)

[1] A. Ali *et al.*, "Review on Recent Progress in Magnetic Nanoparticles: Synthesis, Characterization, and Diverse Applications," Jul. 13, 2021, *Frontiers Media S.A.* doi: 10.3389/fchem.2021.629054.

[2] A. Ali *et al.*, "Review on Recent Progress in Magnetic Nanoparticles: Synthesis, Characterization, and Diverse Applications," Jul. 13, 2021, *Frontiers Media S.A.* doi: 10.3389/fchem.2021.629054.

[3] O. Dos and S. Cavdar, "Impact of Diverse Nanostructure Forms of $NiCo_2O_4$ Bulk Ceramics on Electrical Properties," *ACS Omega*, vol. 10, no. 17, pp. 17875–17886, May 2025, doi: 10.1021/acsomega.5c00708.

[4] S. Rashidi Dafeh, P. Iranmanesh, and P. Salarizadeh, "Fabrication, optimization, and characterization of ultra-small superparamagnetic Fe $_3$ O $_4$ and biocompatible Fe $_3$ O $_4$ @ZnS core/shell magnetic nanoparticles: Ready for biomedicine applications," *Materials Science and Engineering C*, vol. 98, pp. 205–212, May 2019, doi: 10.1016/j.msec.2018.12.147.

[5] G. F. Stiufiuc and R. I. Stiufiuc, "Magnetic Nanoparticles: Synthesis, Characterization, and Their Use in Biomedical Field," Feb. 01, 2024, *Multidisciplinary Digital Publishing Institute (MDPI)*. doi: 10.3390/app14041623.

[6] L. Mandal, Vidya, B. Verma, J. Rani, and P. K. Patel, "Progressive advancement of ZnS-based

quantum dot LED," Jan. 01, 2021, *Springer*. doi: 10.1007/s11082-020-02653-6.

[7] T. Pandey, A. Singh, R. S. Kaundal, and V. Pandey, "Cation exchange doping by transition and non-transition metals: embracing luminescence for band gap tunability in a ZnS lattice," Dec. 06, 2023, *Royal Society of Chemistry*. doi: 10.1039/d3nj05285k.

[8] M. Dile *et al.*, "Evolution of ZnS:Cu nanoparticle morphology during microwave-assisted hydrothermal synthesis," *Nano-Structures and Nano-Objects*, vol. 41, Feb. 2025, doi: 10.1016/j.nanoso.2025.101450.

[9] L. Mandal, Vidya, B. Verma, J. Rani, and P. K. Patel, "Progressive advancement of ZnS-based quantum dot LED," Jan. 01, 2021, *Springer*. doi: 10.1007/s11082-020-02653-6.

[10] A. Goudarzi, S. M. Langroodi, M. Arefkhani, and N. Samadani Langeroodi, "Study of optical properties of ZnS and MnZnS (ZnS/MnS) nanostructure thin films; Prepared by microwave-assisted chemical bath deposition method," *Mater Chem Phys*, vol. 275, Jan. 2022, doi: 10.1016/j.matchemphys.2021.125103.

[11] M. Bhushan, R. Jha, R. Bhardwaj, and R. Sharma, "Visible light emission and enhanced electrocatalytic activity of pure ZnS nanoparticles synthesized via thermal decomposition route", doi: 10.1007/s12034-021-02546-8S.

[12] S. Kumar, M. Singhal, and J. K. Sharma, "Functionalization and characterization of ZnS quantum dots using biocompatible l-cysteine," *Journal of Materials Science: Materials in Electronics*, vol. 24, no. 10, pp. 3875–3880, Oct. 2013, doi: 10.1007/s10854-013-1332-x.

[13] D. Nayak and R. B. Choudhary, "Augmented optical and electrical properties of PMMA-ZnS nanocomposites as emissive layer for OLED applications," *Opt Mater (Amst)*, vol. 91, pp. 470–481, May 2019, doi: 10.1016/j.optmat.2019.03.040.

[14] D. D. Zhang, J. L. Xu, and H. B. Sun, "Toward High Efficiency Organic Light-Emitting Diodes: Role of Nanoparticles," Mar. 01, 2021, *John Wiley and Sons Inc*. doi: 10.1002/adom.202001710.

[15] N. Dudchenko, S. Pawar, I. Perelshtein, and D. Fixler, "Magnetite Nanoparticles: Synthesis and Applications in Optics and Nanophotonics," Apr. 01, 2022, *MDPI*. doi: 10.3390/ma15072601.

[16] X. Cheng *et al.*, "Efficiency enhancement of organic light-emitting diodes with multifunctional magnetic composite nanoparticles of Fe_3O_4@Au@SiO_2," *J Organomet Chem*, vol. 1011, May 2024, doi: 10.1016/j.jorganchem.2024.123123.

[17] S. P. Mucur, B. Canımkurbey, and A. D. Korkmaz, "Magnetic field implementing into the electroluminescence of oled devices doped with $CoFe_2O_4$ nanoparticles," *Light and Engineering*, vol. 28, no. 2, pp. 95–105, 2020, doi: 10.33383/2019-021.

[18] S. G. Meng, X. Z. Zhu, D. Y. Zhou, and L. S. Liao, "Recent Progresses in Solution-Processed Tandem Organic and Quantum Dots Light-Emitting Diodes," Jan. 01, 2023, *MDPI*. doi: 10.3390/molecules28010134.

[19] S. Sim *et al.*, "Universally patternable laser-reduced graphene oxide and polymer blended film for black matrix applications," *Diam Relat Mater*, vol. 158, Oct. 2025, doi: 10.1016/j.diamond.2025.112641.

[20] J. H. Bae *et al.*, "Acid-Base Reaction-Assisted Quantum Dot Patterning via Ligand Engineering and Photolithography," *ACS Appl Mater Interfaces*, vol. 14, no. 42, pp. 47831–47840, Oct. 2022, doi: 10.1021/acsami.2c10297.

[21] M. Noori, M. R. Jafari, S. M. Hosseini, and Z. Shahedi, "Synthesis of Ferrite Nickel Nano-particles and Its Role as a p-Dopant in the Improvement of Hole Injection of an Organic Light-Emitting Diode," *J Electron Mater*, vol. 46, no. 7, pp. 4093–4099, Jul. 2017, doi: 10.1007/s11664-017-5341-z.

[22] H. Lian *et al.*, "Magnetic nanoparticles/PEDOT:PSS composite hole-injection layer for efficient organic light-emitting diodes," *J Mater Chem C Mater*, vol. 6, no. 18, pp. 4903–4911, 2018, doi: 10.1039/c7tc05554d.

[23] M. J. Jacinto, L. F. Ferreira, and V. C. Silva, "Magnetic materials for photocatalytic applications—a review," Oct. 01, 2020, *Springer*. doi: 10.1007/s10971-020-05333-9.

[24] H. Karimi, H. R. Rajabi, and L. Kavoshi, "Application of decorated magnetic nanophotocatalysts for efficient photodegradation of organic dye: A comparison study on photocatalytic activity of magnetic zinc sulfide and graphene quantum dots," *J Photochem Photobiol A Chem*, vol. 397, Jun. 2020, doi: 10.1016/j.jphotochem.2020.112534.

[25] G. Palanisamy, K. Bhuvaneswari, G. Bharathi, T. Pazhanivel, A. N. Grace, and S. K. K. Pasha, “Construction of magnetically recoverable ZnS–WO_3–$CoFe_2O_4$ nanohybrid enriched photocatalyst for the degradation of MB dye under visible light irradiation,” *Chemosphere*, vol. 273, Jun. 2021, doi: 10.1016/j.chemosphere.2021.129687.

[26] C. J. Chang, Z. Lee, K. W. Chu, and Y. H. Wei, “$CoFe_2O_4$ @ZnS core–shell spheres as magnetically recyclable photocatalysts for hydrogen production,” *J Taiwan Inst Chem Eng*, vol. 66, pp. 386–393, Sep. 2016, doi: 10.1016/j.jtice.2016.06.033.

[27] A. Das *et al.*, “Yellow emitting Fe3O4/ZnS hybrid: A probe for in-vitro dermatoglyphics and anti-counterfeiting applications,” *Mater Res Bull*, vol. 131, Nov. 2020, doi: 10.1016/j.materresbull.2020.110966.

[28] D. Ayu Larasati *et al.*, “Green synthesis of $CoFe_2O_4$ /ZnS composite nanoparticles utilizing Moringa Oleifera for magnetic hyperthermia applications,” *Results in Materials*, vol. 19, Sep. 2023, doi: 10.1016/j.rinma.2023.100431.

[29] X. Zhang, B. Tang, Y. Li, C. Liu, P. Jiao, and Y. Wei, “Molecularly imprinted magnetic fluorescent nanocomposite-based sensor for selective detection of lysozyme,” *Nanomaterials*, vol. 11, no. 6, Jun. 2021, doi: 10.3390/nano11061575.

[30] D. Diaz-Diestra, B. Thapa, J. Beltran-Huarac, B. R. Weiner, and G. Morell, “L-cysteine capped ZnS:Mn quantum dots for room-temperature detection of dopamine with high sensitivity and selectivity,” *Biosens Bioelectron*, vol. 87, pp. 693–700, Jan. 2017, doi: 10.1016/j.bios.2016.09.022.

[31] E. Aşik, Y. Akpinar, N. Tülin Güray, M. Işcan, G. Ç. Demircigil, and M. Volkan, “Cellular uptake, genotoxicity and cytotoxicity of cobalt ferrite magnetic nanoparticles in human breast cells,” *Toxicol Res (Camb)*, vol. 5, no. 6, pp. 1649–1662, 2016, doi: 10.1039/c6tx00211k.

[32] M. B. Cánchig *et al.*, “Enhanced selectivity of carbon quantum dots for metal ion detection through surface modification by heteroatom doping: A study on optical properties and theoretical approach,” *Carbon Trends*, vol. 18, Jan. 2025, doi: 10.1016/j.cartre.2024.100445.

[33] J. Liu *et al.*, “Concentration-Dependent Photoluminescence of Carbon Quantum Dots Useable in LED,” *Langmuir*, vol. 40, no. 41, pp. 21524–21532, Oct. 2024, doi: 10.1021/acs.langmuir.4c02413.

[34] Z. Mohammadi, N. Attaran, A. Sazgarnia, S. A. M. Shaegh, and A. Montazerabadi, “Superparamagnetic cobalt ferrite nanoparticles as T2 contrast agent in MRI: In vitro study,” *IET Nanobiotechnol*, vol. 14, no. 5, pp. 396–404, Jul. 2020, doi: 10.1049/iet-nbt.2019.0210.

[35] V. V. Ghazaryan, G. Giester, V. S. Minkov, E. V. Boldyreva, and A. M. Petrosyan, “L-Cysteinium···L-Cysteine Phosphite,” *Journal of Structural Chemistry*, vol. 65, no. 6, pp. 1253–1261, Jun. 2024, doi: 10.1134/S0022476624060131.

[36] Anchal *et al.*, “Tailoring quantum dots through citric acid modulation of $CoFe_2O_4$ ferrite,” *Mater Chem Phys*, vol. 313, Feb. 2024, doi: 10.1016/j.matchemphys.2023.128820.

[37] M. U. Saleem *et al.*, “Study of Kinetics and the Working Mechanism of Silica-Coated Amino-Functionalized $CoFe_2O_4$ Ferrite Nanoparticles to Treat Wastewater for Heavy Metals,” *ACS Omega*, 2023, doi: 10.1021/acsomega.3c07200.

[38] A. B. Alwany *et al.*, “Annealing temperature effects on the size and band gap of ZnS quantum dots fabricated by co-precipitation technique without capping agent,” *Sci Rep*, vol. 13, no. 1, Dec. 2023, doi: 10.1038/s41598-023-37563-6.

[39] V. Alagarsamy *et al.*, “NiS-ZnS quantum dots as visible-light photocatalysts for enhanced dye degradation in sustainable wastewater treatment,” *Chemical Physics Impact*, vol. 11, Dec. 2025, doi: 10.1016/j.chphi.2025.100912.

[40] M. A. Booth, K. Kannappan, A. Hosseini, and A. Partridge, “In-Depth Electrochemical Investigation of Surface Attachment Chemistry via Carbodiimide Coupling,” *Langmuir*, vol. 31, no. 29, pp. 8033–8041, Jul. 2015, doi: 10.1021/acs.langmuir.5b01863.